

Synthesis of new epoxy glucose derivatives as inhibitor for mild steel corrosion in 1.0 M HCl, Experimental study: Part -1

A. Koulou^(a), M. Rbaa^(b), N. Errahmany^(a), F. Benhiba^(c, d), Y. Lakhrissi^(b), R. Tourir^(e), B. Lakhrissi^(b), A. Zarrouk^(d), M. S. Elyoubi^(a)

^(a) Materials Engineering and Environment Laboratory: Modeling and Application, Faculty of Science, University Ibn Tofail P.O. Box 133-14000, Kenitra, Morocco.

^(b) Agro-Resources, Polymers and Process Engineering Laboratory, Department of Chemistry, Faculty of Science, Ibn Tofail University, P.O. Box 133, 14000, Kenitra, Morocco.

^(c) Laboratory of Separation Processes, Department of Chemistry, Faculty of Science, Ibn Tofail University, PO Box 133, 14000, Kenitra, Morocco.

^(d) Materials, Nanotechnology and Environment Laboratory, Faculty of Sciences, Mohammed V University, Av. Ibn Battouta, P.O. Box 1014 Agdal-Rabat, Morocco.

^(e) Regional Center for Education and Training Professions (CRMEF), Kenitra, Morocco.

Abstract

A two non-toxic biodegradable epoxy glucose derivatives, namely 5,6-anhydro-3-O-octa-1,2-O-isopropylidene- α -D-glucofuranose (EGC8) and 5,6-anhydro-3-O-butadecyl-1,2-O-isopropylidene- α -D-glucofuranose (EGC14), were prepared and characterized by using spectroscopic measurements. These products were tested for mild steel corrosion inhibition in 1.0 M HCl using electrochemical measurements. It is shown that these epoxy glucose derivatives affect the cathodic branches with a shift in the cathodic direction (cathodic - type). So, it found that their inhibition efficiency arise with concentrations to achieve a maximum of 93.2 % and 93.48 % at 10⁻³ M of EGC8 and EGC14, respectively, and they depends to the carbon number chain following the order : EGC14 > EGC8. Indeed, it is found that these compounds adsorb according the Langmuir's adsorption isotherm. On the other hand, the temperature effect on the inhibition efficiency of the epoxy glucose derivatives indicated that they take them at high-rise temperature. In addition, the calculated kinetic and thermodynamic parameters have shown that EGC8 act via physical adsorption while EGC14 act via chemical adsorptions, and their process are endothermic and spontaneous.

* Corresponding author:

touir8@gmail.com

Received 02 April 2020,

Revised 26 June 2020,

Accepted 28 June 2020.

Keywords: Synthesis and characterization; Epoxy glucose derivatives; Inhibition of mild steel corrosion; Molar hydrochloric acid; Electrochemical measurements

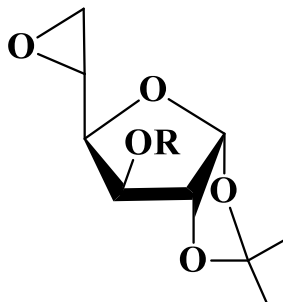
1. Introduction

The protection of iron and its alloys against corrosion in acidic solutions became very important. So, the hydrochloric acid was often used many application industries such as pickling bath which used to remove undesirable corrosion products causing also a metal degradation upon the already cleaned surface [1,2]. To prevent this problem, several organic compounds have been used [3,4]. Generally, most organic compounds contain heteroatoms such as nitrogen (-N), sulfur (-S), and/or oxygen (-O) atoms [5,6]. They may be adsorb and block the active sites on metallic surface and consequently decrease its corrosion rate [7]. So, it is found that the mechanism action of the organic compounds will be affected by their molecular structure, chemical composition of solution, surface metal charge and other factors [8]. Recently, many researches were carried out to develop a new non-toxic corrosion inhibitors and biodegradable such as sodium gluconate [9-11], bis-glucobenzimidazolones derivatives [12], anhydrous tricalcium phosphate [13], and monosaccharides [14, 15]. For these last products, it is found that their inhibition efficiency depends to their concentrations and molecular structures. In this study two new non-toxic and biodegradable epoxy glucose derivatives compounds were synthesized and identified by using spectroscopic measurements. These compounds were investigated as corrosion inhibitors for mild steel in molar hydrochloric acid (1.0 M HCl) using electrochemical measurements. The influence of temperature solution was also investigated and discussed.

2. Material and Methods

2.1. Electrolytic cell, inhibitors and materials

The molecular structures of the tested epoxy glucose derivatives are shown in Figure 1:



Where EGC8 ($R = -C_8H_{17}$) and EGC14 ($R = -C_{14}H_{29}$).

Figure 1: Molecular structure of the tested inhibitors.

So, the corrosive solution of molar hydrochloric solution (1.0 M HCl) was prepared using distillate water (an analytical grade chemical product was used). An electrolytic cell with a standard three-electrode was made for electrochemical study using Potentiostat/Galvanostat/Voltalab PGZ 100. The used working electrode had the following chemical composition (in wt. %): 0.11 C, 0.24 Si, 0.47 Mn, 0.12 Cr, 0.02 Mo, 0.1 Ni, 0.03 Al, 0.14 Cu, 0.06 W, <0.0012 Co, <0.003 V, and 98.6658 Fe. This electrode was embedded in a polyester resin to expose an active area of 1 cm². Before each immersion test, the tested electrode surface was abraded with abrading paper (size of grain is from 200 to 1200), cleaned with acetone, washed with distilled water, and finally dried in hot air. All values of the potentials and current densities were measured versus reference electrode of saturated calomel (SCE) and an auxiliary electrode of platinum plate, respectively.

2.2. Current – Potential measurements

For electrochemical tests, the mild steel electrode is immersed in the corrosive solution for 1 h at open circuit potential (E_{OCP}). The cathodic and anodic branches have been traced by polarization of the E_{OCP} in the direction of a more negative and positive direction respectively, with a scanning speed of 0.5 mV/s (this tests are carried out three times

independent for each concentration). To extract the electrochemical corrosion parameters, an adjusting using Stern–Geary equation was used [16] as indicated in the previous works [17, 18]. The inhibition efficiency (η_{pp}) and the coverage values (θ) were determined using the following equations:

(1)

$$\theta = 1 - \frac{i_{corr}}{i_{corr}^0} \quad (2)$$

where i_{corr}^0 and i_{corr} are the corrosion current density values in the absence and presence of each epoxy glucose, respectively.

2.3. Electrochemical impedance measurements

Electrochemical impedance spectroscopy was plotted at E_{OCP} over frequency interval from 100 kHz to 0.1 Hz with 10 points/decade and an amplitude of the AC signal of 10 mV_{rms}. The obtained impedance spectrum were simulated using EC-Lab software.

3. Results and discussions

3.1. Identification of the tested compounds

The characterization of the obtained compounds are presented below :

- Characterization of inhibitor C_8H_{17} (EGC8):

Yield: 85 %; Brute formula ($C_{17}H_{30}O_5$), Mm = 314,42 (g/ mol); FT-IR (KBr, cm^{-1}): 2866-2930 (2 CH_3), 1470 (CH), 1180 (C-O), 748 (CH_2). 1H NMR (300 MHz, DMSO- d_6) (δ ppm): 0.90 (s, 3 H, CH_3), 1.20 (d, 6 H, 2 CH_3), 3.50-5.47 (d, 4 H, CH-glucose function). ^{13}C NMR (75 MHz, DMSO- d_6) (δ ppm): (111.02)2 $C(CH_3)_2$, 24.25, 26.25 (2 $C(CH_3)_2$), 13.20 (CH_3), 68.50-81.021 (CH-glucose function).

- Characterization of inhibitor $C_{14}H_{29}$ (EGC14):

Yield: 75 %; Brute formula ($C_{23}H_{42}O_5$), Mm = 398,58 (g/ mol); FT-IR (KBr, cm^{-1}) ν : 2817-2929 (2- CH_3), 1376 (CH), 1267 (C-O), 780 (CH_2). 1H NMR (300 MHz, DMSO- d_6) (δ ppm): 0.81 (s, 3 H, CH_3), 3.14-3.18 (m, 31 H, CH_2 -carbon chain), 1.17, 1.80 (d, 6 H, 2 CH_3), 3.36-4.02 (d, 4 H, CH-glucose function). ^{13}C NMR (75 MHz, DMSO- d_6) (δ ppm): (113.13), 2 $C(CH_3)_2$ 25.68, 27.79 (2 $C(CH_3)_2$), 13.29 (CH_3 -carbon chain), 81.08-82.77 (CH-glucose function). 28.49-30.10 (CH-carbon chain).

3.2. Electrochemical study

3.2.1. Open circuit potential evolution

Figure 3 represents the evolution of the potential at the open circuit (E_{OCP}) versus immersion time at various concentrations of EGC8 or EGC14. It can be seen that the E_{OCP} for the free-solution decreases with time to stabilize at - 545 mV/SCE after one hour. This finding may be related to the dissolution of the surface of the mild steel electrode with the formation of hydroxyl and/or hydroxide iron (corrosive products) on its surface. Thus, it should be noted that the displacement of the potentials in the anodic direction becomes (ennobling of the potential) quickly stable with immersion time, in the presence of EGC8 or EGC14. This result can be attributed to the formation of a protective layer by the inhibitor molecules on the mild steel surface.

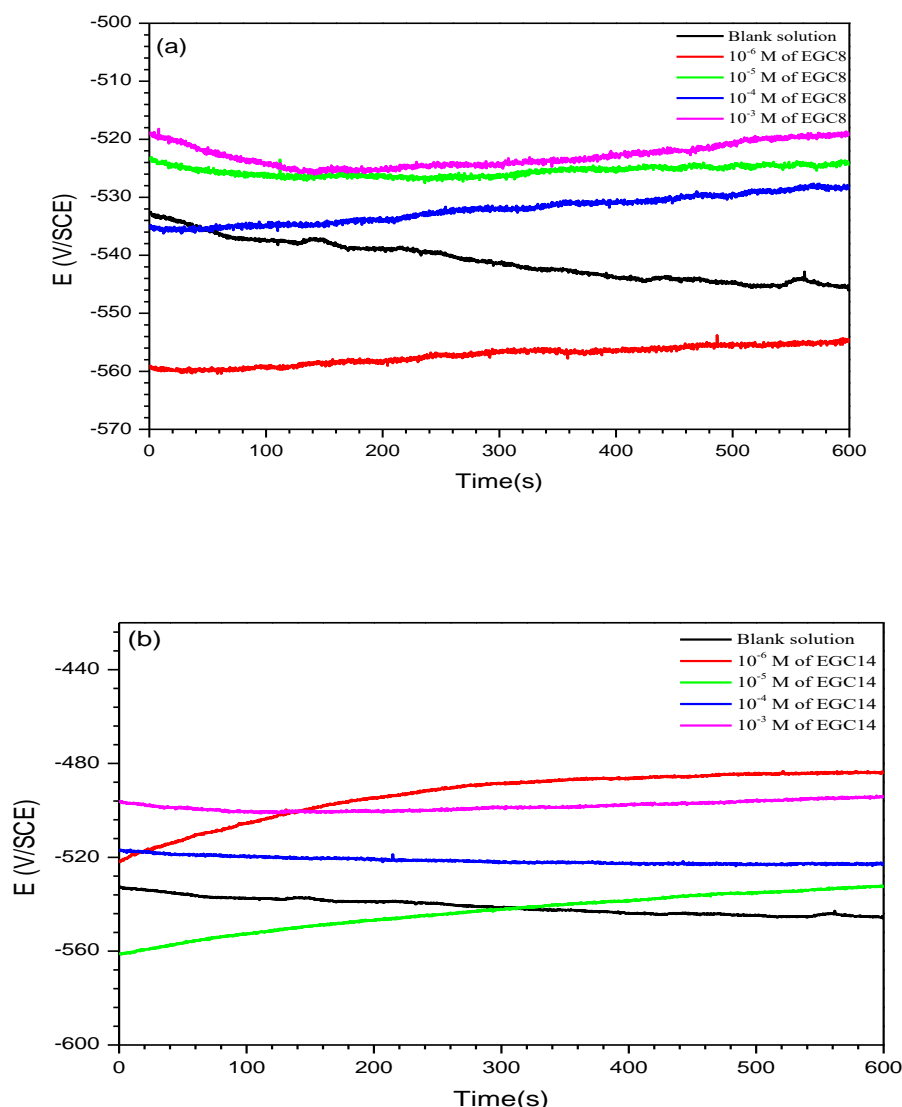


Figure 2 : Evolution of the potentials at the open circuit, E_{OCP} , versus time for mild steel electrode in corrosive solution at various concentrations of (a) EGC8 and (b) EGC14.

3.2.2. Impedance spectroscopy evaluation

Figure 3 represents the obtained Nyquist impedance plots for mild steel in corrosive solution after 1 h of immersion time at E_{OCP} at various concentrations of non-toxic inhibitors, EGC8 or EGC14. It is seen that all plots are composed of a single no-ideal capacitive loop. This deviation was generally corresponded to the frequency dispersion because of heterogeneous surface, adsorption of inhibitors molecules, and other states [19, 20]. For this, the simulation using constant phase elements (CPE) rather than an ideal capacitor was recommended [21] by using the equivalent electrical circuit (Figure 4) which generally used to describe the iron/acid interface [22]. However, for the evaluation of the inhibition efficiency, the values of the polarization resistance (R_p) were used (equation 5). This resistance composes by the value of the resistance of the charge transfer, R_{ct} (which represents the resistance between the metal/external Helmholtz planes) and the resistance of the diffuse layer (R_d) containing accumulated species and other products (R_a), etc. on the metallic surface such as reported in literature [23–25]. In addition, the CPE element represents all the frequency of electrochemical phenomena depending such as indicated above [26, 27] and its impedance as follow :

$$CPE = \frac{1}{Y_0(j\omega)^n} \quad (3)$$

Where Y_0 is the magnitude of the CPE, j is the imaginary number, $\omega = 2\pi f$ is the angular frequency (rad s^{-1}), n is the exponent of CPE (number of $n = 1, 0$, or -1). So, this element (CPE or Q) has been used (in place of the double layer capacitance, C_{dl}) in order to precisely adjust the experimental data [28, 29]. Indeed, the value of C_{dl} derived from the CPE parameters using the following equation [30] :

$$C_{dl} = Q^{\frac{1}{n}} \times R^{\frac{(1-n)}{n}} \quad (4)$$

Such as mentioned above, the inhibition efficiency (η_{EIS}) was calculated using R_p (which $R_p = R_{ct} + R_d$) :

$$\eta_{EIS} = \frac{R_p - R_p^0}{R_p} \times 100 \quad (5)$$

Where R_p^0 and R_p are the values of the resistance polarization without and with EGC8 or EGC14 at various concentrations, respectively. The electrochemical parameters R_s , R_p , CPE_{dl} , C_{dl} , and n_{dl} were determined by using the EC-Lab software and were indicated in Table 2. It is seen that the values of R_p increase to achieve its maximum at 10^{-3} M for both epoxy glucose while the CPE values decrease to achieve its minimum at the same concentration.

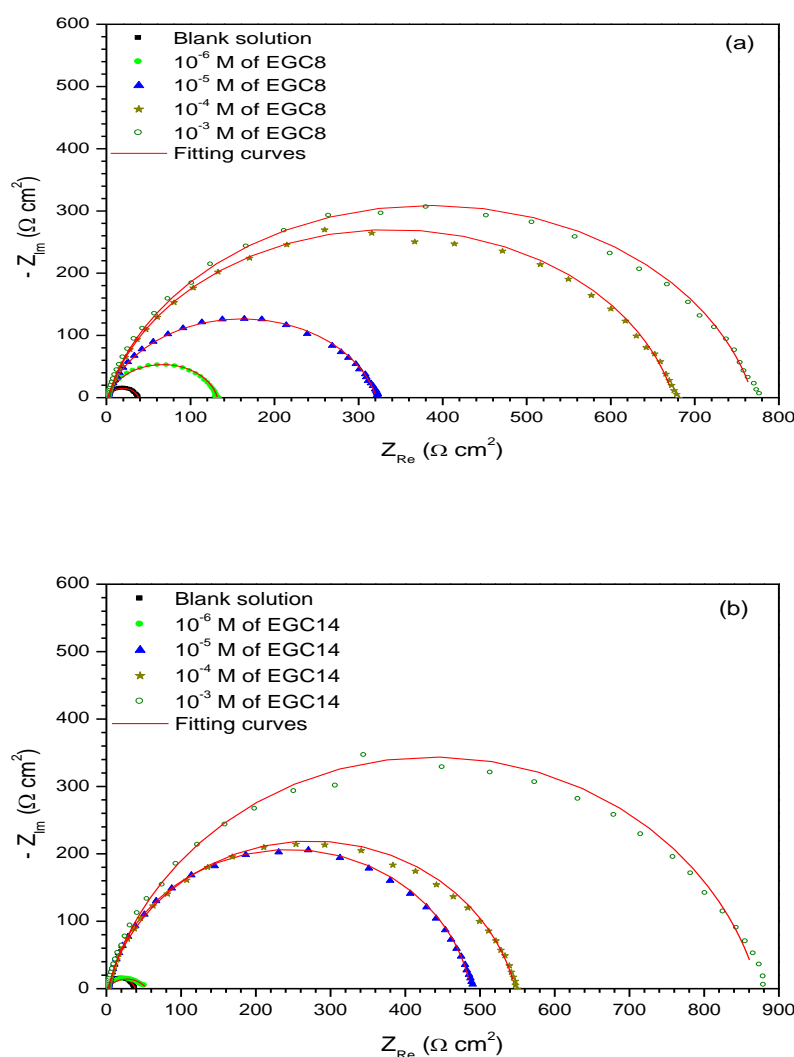


Figure 3: Impedance plots for mild steel in molar hydrochloric solution at E_{OCP} containing different concentrations of (a) EGC8 and (b) EGC14. ($T = 298 \text{ K}$).

This result can be explained by the protection of the metal surface by the formation of a resistive layer by the epoxy glucose molecules. The same results in the literature which can be explained by the adsorption of inhibitor molecules

on the metallic surface or by the increase in the ply of the formed layer at the metal/electrolyte interface [31, 32]. On the other hand, it should be noted that the values of n_{dl} raise with the concentration for both compounds. This effect can be interpreted by the increase of homogeneity of mild steel surface resulting from the formation of a protective layer by the adsorption of molecules of the epoxy glucose on the metallic surface [33, 34].

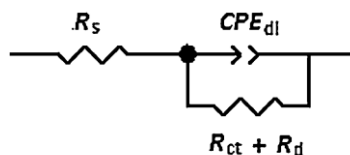


Figure 4: Proposed equivalent electrical circuit.

Table 4: Electrochemical data and inhibition efficiencies values for mild steel in molar hydrochloric with various concentrations of EGC8 or EGC14 at 298 K.

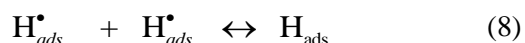
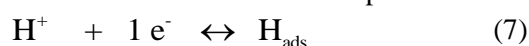
	C (M)	$R_s(\Omega \text{ cm}^2)$	$R_{ct}+R_d(\Omega \text{ cm}^2)$	$CPE_{dl}(\mu F \text{ s}^{n-1})$	$C_{dl}(\mu F \text{ cm}^{-2})$	n_{dl}	$\eta_{EIS}(\%)$
Free solution	00	2.08 ± 0.03	32.41 ± 0.78	1100.69 ± 0.66	128.1 ± 0.66	0.78 ± 0.01	-
EGC8	10^{-6}	2.66 ± 0.05	130.01 ± 0.64	102.10 ± 4.76	54.91 ± 0.21	0.87 ± 0.05	84.03
	10^{-5}	1.46 ± 0.03	339.70 ± 0.43	90.04 ± 0.41	67.63 ± 0.41	0.78 ± 0.01	86.72
	10^{-4}	1.68 ± 0.01	673.20 ± 0.44	67.07 ± 0.49	40.73 ± 0.34	0.86 ± 0.06	90.06
	10^{-3}	1.65 ± 0.02	768.10 ± 0.43	66.05 ± 0.44	41.06 ± 0.31	0.87 ± 0.05	93.20
	10^{-6}	0.43 ± 0.05	53.39 ± 0.36	776.70 ± 7.31	11.05 ± 0.31	0.77 ± 0.08	84.26
EGC14	10^{-5}	0.88 ± 0.03	320.40 ± 0.44	100.20 ± 1.00	48.66 ± 0.08	0.85 ± 0.01	88.39
	10^{-4}	1.65 ± 0.14	545.51 ± 0.43	68.90 ± 0.64	40.66 ± 0.54	0.86 ± 0.06	90.66
	10^{-3}	2.15 ± 0.19	871.00 ± 0.40	88.17 ± 0.44	56.04 ± 0.18	0.85 ± 0.01	93.48

3.2.3. Potentiodynamic polarization evaluation

Figure 5 shows the current – potential curves of mild steel in molar hydrochloric solution at various concentrations of EGC8 and EGC14 at 298 K and their extracted parameters are presented in Table 5. According to the literature, the reaction of the oxidation of mild steel in acidic medium takes place according to the below equation [35]:



When the main reaction is the proton reduction reaction on steel following the Volmer-Heyrovsky equation [36, 37]:



However, it should be noted that the β_c values not significantly change with epoxy glucose derivatives addition indicating no change in the proton reduction mechanism (Table 5). This result suggested that the inhibition action of EGC8 and EGC14 molecules occurs with simple blocking of the site of the surface of electrode, causing a decrease its active site without changing on the mechanism of reduction reaction [38, 39]. The curves of the anodic currents were slightly changed with the inhibitor concentrations showing a change in the oxidation reaction of the mild steel. On the other hand, it should be noted that the values of anodic and cathodic current densities take down in the presence of EGC8 or EGC14 compared to the blank solution with a shift of the corrosion potential values (E_{corr}) to the cathodic direction. These results indicate that these epoxy glucose derivatives act as cathodic -type inhibitor. Indeed, it is remarked in the anodic part, beyond the potential value of - 0.310 V/SCE, the presence of inhibitors did not affect the current- potential curves. This potential called the desorption potential where the inhibition action of the tested

compounds is related to the potential of electrode. From Table 4, it can be observed that the inhibition efficiency, η_{pp} %, rises with concentration to get a maximum value of 92.12 % and 96.01 % at 10^{-3} M of EGC8 and EGC14, respectively. This increase can be interpreted by the state of the layer formed on the surface of the metal which has become more resistive at higher concentrations by the adsorption of the molecules of the tested inhibitors on the metallic surface.

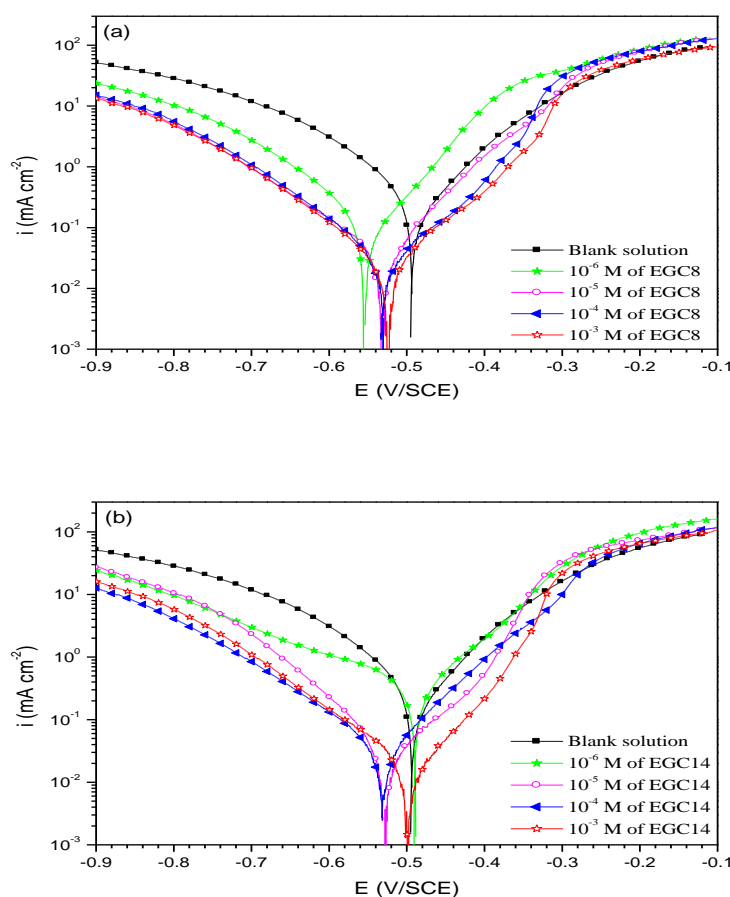


Figure 5: Current – potential curves traced for mild steel in molar hydrochloric acid at various concentrations of (a) EGC8 and (b) EGC14 ($T = 298$ K).

Table 5: Electrochemical data and inhibition efficiencies values for mild steel in molar hydrochloric acid at various concentrations of EGC8 or EGC14 ($T = 298$ K).

	C (M)	E_{corr} (mV/SCE)	i_{corr} ($\mu A\ cm^{-2}$)	$-\beta_c$ (mV dec^{-1})	β_a (mV dec^{-1})	η_{pp} (%)
Free solution	00	-545.12 ± 0.54	712.23 ± 0.17	101.13 ± 0.17	98.13 ± 0.15	-
EGC8	10^{-6}	-555.48 ± 0.50	235.47 ± 0.07	137.40 ± 0.36	77.00 ± 0.46	84.75
	10^{-5}	-531.97 ± 0.31	42.13 ± 0.40	124.14 ± 0.88	96.12 ± 0.18	85.82
	10^{-4}	-530.30 ± 0.21	43.01 ± 0.40	121.52 ± 0.34	71.32 ± 0.21	87.53
	10^{-3}	-525.05 ± 0.14	30.37 ± 0.30	117.75 ± 0.02	77.00 ± 0.02	92.12
EGC14	10^{-6}	-488.41 ± 0.11	478.82 ± 0.05	115.71 ± 0.83	88.91 ± 0.24	84.62
	10^{-5}	-530.45 ± 0.36	73.04 ± 0.54	112.12 ± 0.12	55.71 ± 0.34	87.83
	10^{-4}	-530.03 ± 0.46	41.86 ± 0.46	130.7 ± 0.51	95.92 ± 0.61	89.39
	10^{-3}	-498.60 ± 0.62	22.24 ± 0.62	118.77 ± 0.67	50.12 ± 0.87	96.01

3.2.4. Temperature effect and activation parameters

Temperature is an essential means for the inhibition and corrosion study of metal, especially in acidic solution. Increasingly, the temperature allows us to determine several activation parameters, in order to obtain the appropriate mode of the adsorption mechanism of the inhibitory molecules on the metal surface. In fact, the effect temperature solution on the mild steel corrosion in molar hydrochloric acid without and with 10^{-3} M of each compound EGC8 or EGC14 and their corresponding extracted parameters are shown in Figure 6 and Table 6, respectively. It should be noted that the rise in the temperature from 298 K to 328 K, caused a positive and negative change in E_{corr} for free solution and in the presence of 10^{-3} M of EGC8 or 10^{-3} M of EGC14, respectively. It has been clearly observed from Figures 6b and 6c, that the current densities in the presence of epoxy glucose derivatives increase with the increase of the temperature solution. The relationship between the apparent energy of activation (E_a), the rate of corrosion (i_{corr}) and the temperature (T) is follow :

$$i_{\text{corr}} = A \exp\left(\frac{-E_a}{RT}\right) \quad (9)$$

where R and A are respectively the gas and the pre-exponential constants. The plots $\ln(i_{\text{corr}})$ vs. $1/T$ were given in Figure 7 where the E_a values without and with 10^{-3} M of EGC8 or EGC14 were determined and the obtained values are presented in Table 6. According to the literature, the pre-exponential constant A (equation 9) is linked to the number of active centers [40] where have different energies. Thus, two possibilities are given: in the case where the activation energy with the addition of inhibitors is greater than in the case of free solution, the inhibitory molecules are adsorbed on the majority of active sites with lower energy and the corrosion reaction takes place mainly on other active sites with high energy. Otherwise, the energy of activation with inhibitors addition is lower in the case of free solution, consequently, a smaller number of active sites remain not covered by inhibitory molecules, which have participated in the process of corrosion. This case is normally obtained when the adsorbed molecule of inhibitor protects the majority of active sites which are the least active [41]. So, in our case, it is noted that the energy of activation, E_a , in the presence of EGC8 or EGC14 is about $51.88 \text{ kJ mol}^{-1}$ and $36.08 \text{ kJ mol}^{-1}$, respectively, where are greater than in their absence which is $21.05 \text{ kJ mol}^{-1}$ suggesting an action of physical adsorption.

In addition, the enthalpy (ΔH_a) and entropy (ΔS_a) of activation were determined by the below equation 10:

$$i_{\text{corr}} = \frac{RT}{Nh} \exp\left(\frac{\Delta S_a}{R}\right) \exp\left(\frac{\Delta H_a}{RT}\right) \quad (10)$$

where h and N are the Plank's and the Avogadro's numbers, respectively. Figure 8 indicates the curves $\ln(i_{\text{corr}}/T)$ against $1000/T$. These curves are linear where by its slope ($-\Delta H_a/R$) and its intercept ($\ln R/Nh + \Delta S_a/R$), the ΔH_a and ΔS_a values may be calculated (the obtained values are presented in Table 6). It is seen that ΔH_a values are positive in all cases indicating that the nature of mild steel corrosion process is endothermic. On the other hand, it is found that the value of the entropies ΔS_a^* for EGC8 and EGC14 is largely negative assuming that the activated complex in the rate determination stage represents an organization rather than a dissociation indicating a reduction in the disorder while the passage of reactants to the activated complex [42-44].

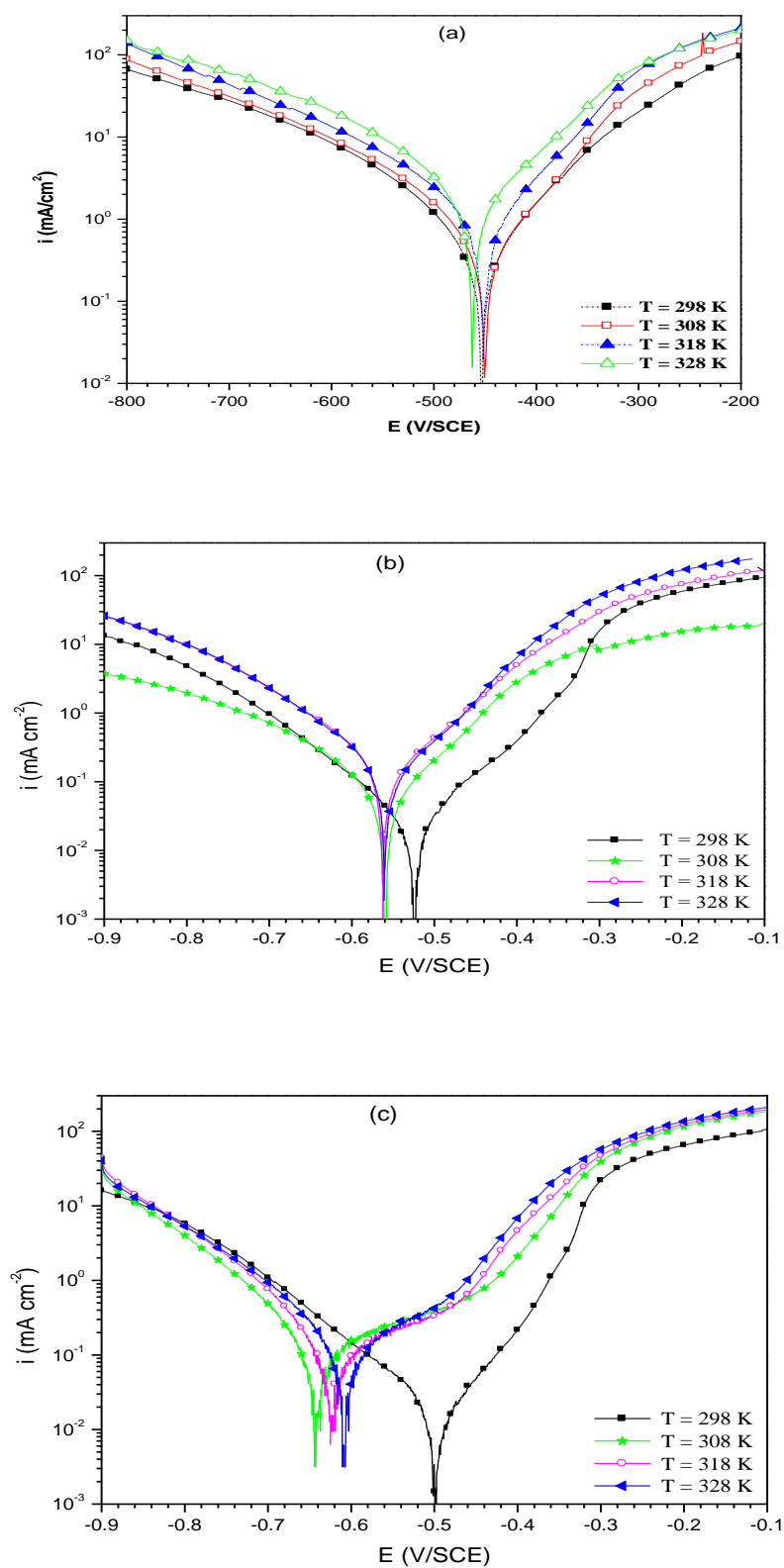


Figure 6 : Cathodic and anodic curves of mild steel in molar hydrochloric acid at various temperatures (a) without inhibitor , and with 10^{-3} M (b) EGC8 or (c) EGC14.

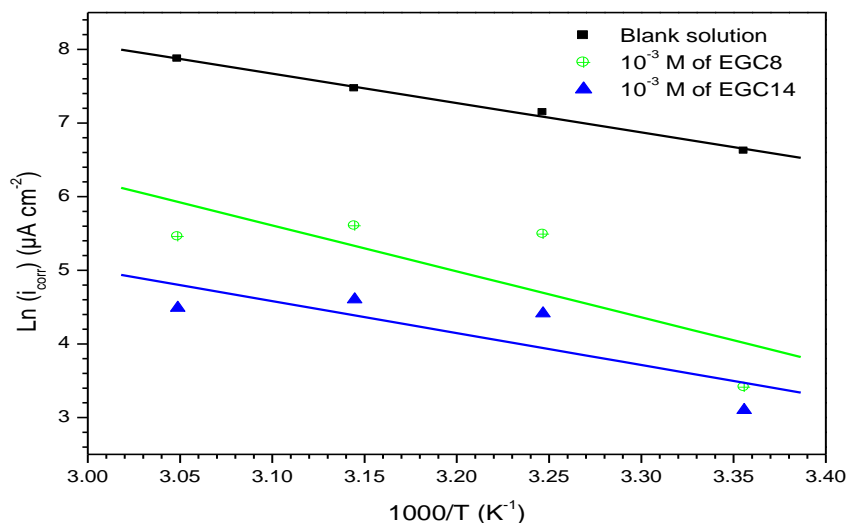


Figure 7: $\text{Ln}(i_{\text{corr}})$ versus $1000/T$ curves of mild steel in molar hydrochloric acid without and with 10^{-3} M of EGC8 or EGC14.

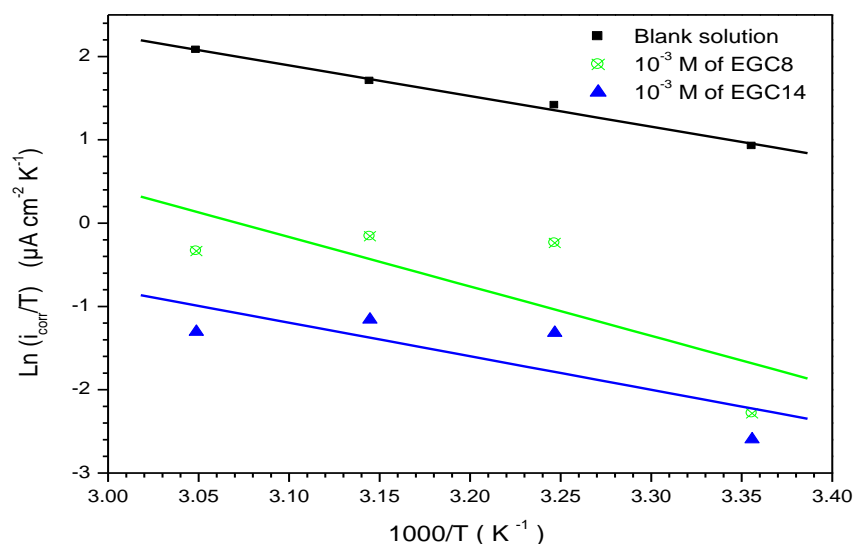


Figure 8: Transitions curves of mild steel corrosion in molar hydrochloric acid without and with 10^{-3} M of EGC8 or EGC14.

3.2.5. Adsorption parameters

The adsorption parameters have several advantages in the corrosion inhibition study by the chemical inhibitors, among them the knowledge of the nature of adsorption [45]. In fact, two principal types of interaction have been used to describe the interactions between the inhibitory molecules and the metal surface : physical and chemical adsorption. So, the adsorption mechanisms of epoxy glucose derivatives EGC8 and EGC14 on the metallic surface were determined by adjusting the coverage surface, θ , values obtained from the current – potential parameters to different adsorption isotherms for 298 K. Thus, the best adjustments were obtained from the Langmuir's adsorption isotherm where the correlation coefficient is equal to 1. Following to this isotherm adsorption, θ is linked to the concentration of inhibitor C_{inh} as follow:

$$\frac{C_{inh}}{\theta} = \frac{1}{K_{ads}} + C_{inh} \quad (11)$$

where K_{ads} is the equilibrium constant of the adsorption process. The obtained plots are presented in Figure 9.

Table 6: Electrochemical and activated thermodynamic parameters of mild steel molar hydrochloric acid without and with 10^{-3} M of EGC8 or EGC14 at various temperature solution values

	T(K)	E_{corr} (mV/SCE)	i_{corr} ($\mu\text{A}/\text{cm}^2$)	E_a (kJ mol^{-1})	ΔH_a (kJ mol^{-1})	ΔS_a ($\text{J mol}^{-1} \text{K}^{-1}$)
Free solution	298±2	-500	750	21.05	18.46	-126.07
	308±2	-487	1266	—	—	—
	318±2	-490	1750	—	—	—
	328±2	-478	2620	—	—	—
10^{-3} M of EGC8	298±2	-525.05	30.37	51.88	49.28	-46.14
	308±2	-560.44	242.67	—	—	—
	318±2	-562,52	271.76	—	—	—
10^{-3} M of EGC14	328±2	-560.17	234.50	—	—	—
	298±2	-498.60	22.24	36.08	33.48	-103.71
	308±2	-641.76	82.54	—	—	—
	318±2	-622.89	99.88	—	—	—
	328±2	-608.88	88.99	—	—	—

The adsorption energy was calculated by the equation 12 :

$$K_{ads} = \frac{1}{55.5} \exp\left(\frac{-\Delta G_{ads}}{RT}\right) \quad (12)$$

According to the literature: The activation energy, lower than -40 kJ / mol shows that the type of adsorption is chemical. If it is greater than - 40 kJ / mol indicates that the adsorption type is physical. If the energy of adsorption value between - 20 kJ / mol and -40 kJ / mol both types of adsorption (physical and chemical) involved [45, 46].

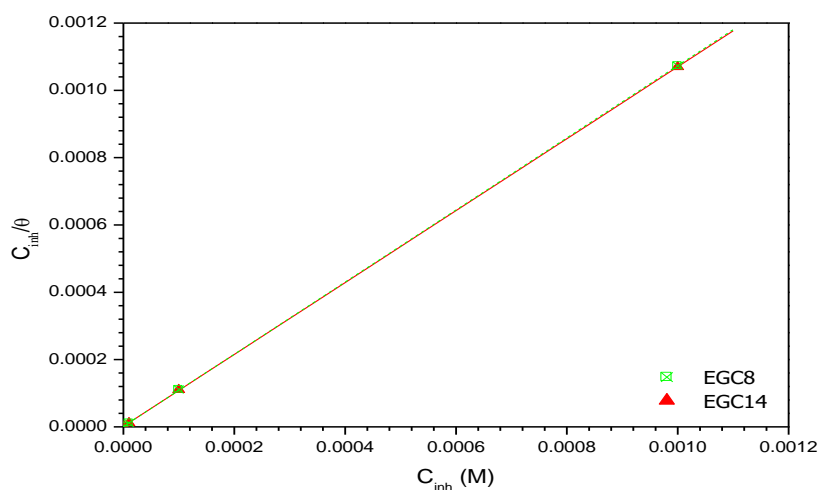


Figure 9: Langmuir's adsorption isotherm plots for mild steel in molar hydrochloric acid at various concentrations of EGC8 or EGC14.

It is found that the adsorption energy values for the EGC8 and EGC14 molecules are - 14 kJ/mol and - 48 kJ/mol, respectively. This finding indicates that the adsorption of EGC8 molecules is the type physical while for EGC14 molecules is the type chemical.

Conclusion

In this study, non-toxic epoxy glucose derivatives were synthesized and characterized. These compounds were investigated for the corrosion resistance for mild steel in molar hydrochloric acid solution (1.0 M HCl). It is shown that these epoxy glucose have good character of inhibition for mild steel corrosion in 1.0 M HCl medium where their inhibition arise with their concentrations to attain about a maximum value of 93 % and 94 % at 10^{-3} M of EGC8 and EGC14, respectively. Therefore, the current – potential study showed that these two products react as cathodic type inhibitors. On the other hand, it is found that these non-toxic compounds adsorb to the metallic surface according to the Langmuir's adsorption isotherm. Finally, it is obtained that both compounds take their performance at higher temperature and their obtained values of the apparent activation and free energies indicating that they act via physical and chemical adsorptions, respectively.

References

- [1] K. Bouyad, Y. Kandri Rodi, H. Elmsellem, E. H. El Ghadraoui, Y. Ouzidan, I. Abdel-Rahman, H.S. Kusuma, I. Warad, J.T. Mague, E.M. Essassi, B. Hammouti, A. Chetouani, Imidazo[4,5-b]pyridines as a New Class of Corrosion Inhibitors for Mild Steel: Experimental and DFT Approach, *Mor. J. Chem.* 6(1) (2018) 22-34
- [2] O. Fergachi, F. Benhiba, M. Rbaa, M. Ouakki, M. Galai, R. Tourir, B. Lakhrissi, H. Oudda, M. Ebn Touhami, *J. Bio- and Tribo-Corrosion*, (2019) 5:21.
- [3] B. Hammouti, B. Aouniti, M. Taleb, M. Brighli, *Corrosion*, 51(6) (1995) 411–416.
- [4] E. Ech-chihbi, R. Salim, H. Oudda, A. Elaattiaoui, Z. Rais, A. Oussaid, M. Taleb, *Der. Pharm. Chem.*, 8(13) (2016) 214–230.
- [5] A. Zouitini, Y. Kandri Rodi, H. Elmsellem Chahdi, H. Steli, C. Ad, Y. Ouzidan, E. M. Essassi, A. Chetouani, B. Hammouti, A. Zouitini, *Mor. J. Chem.* 6(3) (2018) 391-403
- [6] M. Galai, M. Rbaa, Y. Kacimi, M. Ouakki, N. Dkhirech, R. Tourir, M. Ebn Touhami, *Anal. Bioanal. Electrochem.*, 9(1) (2017) 80–101.
- [7] O.K. Abiola, *Corros. Sci.*, 48 (2006) 3078–3090
- [8] K. Benbouya, A. Rochdi, M. El Bakri, H. Larhzil, R. Tourir, M. Ebn Touhami, *J. Mater. Environ. Sci.*, 9 (2018) 2730-2740
- [9] R. Tourir, M. Cenoui, M. El Bakri, M. Ebn Touhami, *Corros. Sci.*, 50 (2008) 1530–1537.
- [10] R. Tourir, M. El Bakri, N. Dkhireche, M. Ebn Touhami, A. Rochdi, *J. Mater. Environ. Sci.*, 1 (S1) (2010) 317-328.
- [11] R. Tourir, N. Dkhireche, M.Ebn Touhami, M. El Bakri, A. Rochdi, R. A. Belakhmima, *J. Saudi Chem. Soc.*, 18 (2014) 873–881
- [12] L. Lakhrissi, B. Lakhrissi, R. Tourir, M. Ebn Touhami, M. Massoui, E. M. Essassi, *Arab. J. Chem.*, 10 (2) (2017) S3142-S3149.
- [13] L. Chafki, E. H. Rifi, R. Tourir, M. Ebn Touhami, Z. Hatim, *Open Mater. Sci. J.*, 12 (2018) 68-81.
- [14] A. Methal, A. Koulou, M. El Bakri, M. Ebn Touhami, M. Galai, M. Lakhrissi, R. Tourir, S. Bakkali, *Maghr. J. Pure & Appl. Sci.*, 1 N° 2 (2015) 46 -61.
- [15] A. Koulou, F. Benhiba, M. Rbaa, N. Errahmany, Y. Lakhrissi, R. Tourir, B. Lakhrissi, A. Zarrouk, M. S. Elyoubi, Synthesis of new epoxy glucose derivatives as inhibitor for mild steel corrosion in 1.0 M HCl: DMol3 theory and molecular dynamics simulation study: Part-2, *Mor. J. Chem.* 8(1) (2020) 157-166
- [16] M. Stern, A. L. Geary, *J. Electrochem. Soc.*, 104(1) (1957) 56–63.

- [17] K. Adardour, R. Touir, M. El Bakri, H. Larhzil, M. EbnTouhami, Y. Ramli, A. Zarrouk, H. El Kafsoui, E. M. Essassi, *Res. Chem. Inter.*, 39(2013) 1843–1855.
- [18] K. Adardour, R. Touir, M. El Bakri, Y. Ramli, M. EbnTouhami, H. El Kafsoui, C. Kalonji Mubengayi, E. M. Essassi, *Res. Chem. Inter.*, 39(2013) 4175–4188.
- [19] M. Behpour, S.M. Ghoreishi, N. Soltani, M. Salavati-Niasari, *Corros. Sci.*, 51 (2009) 1073-1082.
- [20] J. Aljourani, K. Raeissi, M.A. Golozar, *Corros. Sci.*, 51 (2009) 1836-1843.
- [21] C.H. Hsu, F. Mansfeld, *Corrosion* 57, (2001) 747–748
- [22]. J.R. Macdonald, *J. Electroanal. Chem.*, 223 (1987) 25–50
- [23] B.D. Mert, A.O. Yuce, G. Kardas, B. Yazıcı, *Corros. Sci.*, 85 (2014) 287-295.
- [24] H. Keles, M. Keles, *Res. Chem. Intermed.*, 40 (2014) 193-209.
- [25] G. Kardas, R. Solmaz, *Corros. Rev.*, 24(3-4) (2006) 151.
- [26] K.F. Khaled, M.A. Amin, *Corros. Sci.*, 51 (2009) 1964-1975.
- [27] M. Ozcan, I. Dehri, M. Erbil, *Prog. Org. Coat.*, 44 (2002) 279-285.
- [28] F. Bentiss, M. Lebrini, H. Vezin, F. Chai, M. Traisnel, M. Lagrené, *Corros. Sci.*, 51 (2009) 2165-2173.
- [29]. R. Solmaz, *Corros. Sci.*, 52 (2010) 3321-3330.
- [30] H. Gerengi, K. Darowicki, G. Bereket, P. Slepiski, *Corros. Sci.*, 51(11) (2009) 2573-2579.
- [31] R. Solmaz, *Corros. Sci.*, 79 (2014) 169-176.
- [32] A. Espinoza-Vazquez, G.E. Negron-Silva, R. Gonzalez-Olvera, D. Angeles-Beltran, H. Herrera-Hernandez, M. Romero-Romo, M. Palomar-Pardave, *Mater. Chem. Phys.*, 145 (3)(2014) 407-417.
- [33] R. Khriouf, M. Galai, H. El Bakri, H. Larhzil, R. Touir, M. Ebn Touhami, Y. Ramli, *Chem. Data Collec.*, 24 (2019) 100303
- [34] A. Rochdi, R. Touir, M. El Bakri, M. Ebn Touhami, S. Bakkali, B. Mernari, *J. Env. Chem. Eng.*, 3 (2015) 233-242.
- [35] A. Majjane, D. Rair, A. Chahine, M. Et-tabirou, M. Ebn Touhami, R. Touir, *Corros. Sci.*, 60 (2012) 98–103.
- [36] K. Adardour, O. Kassou, R. Touir, M. Ebn Touhami, H. ElKafsoui, H. Benzeid, E. M. Essassi, M. Sfaira, *J. Mater. Environ. Sci.*, 1 (2) (2010) 129-138.
- [37] R. Touir, R. A. Belakhmima, M. Ebn Touhami, L. Lakhrissi, M. El Fayed, B. Lakhrissi, E. M. Essassi, *J. Mater. Environ. Sci.*, 4(6) (2013) 921-930
- [38] M. Zerfaoui, H. Oudda, B. Hammouti, S. Kertit, M. Benkaddour, Inhibition of corrosion of iron in citric acid media by aminoacids, *Progress in Organic Coatings*, 51 (2004) 134-138
- [39] L. El Ghayati, A. Batah, M. Belkhaouda, L. Bammou, R. Salghi, A.Saber, A. Chetouani, M.L. Taha, E.M. Essassi, Experimental and theoretical investigation of 4-Methyl-2,3-dihydro-1H-1,5-benzodiazepin-2-one on the corrosion and inhibition behavior of steel in acidic solution, *Mor. J. Chem.* 7(3) (2019) 567-579
- [40] A. Ali Gurten, Hulya Keles, Emel Bayol, Fatma Kandemirli, *J. Indus. Eng. Chem.*, 27 (2015) 68–78.
- [41] M. Bouklah, B. Hammouti, M. Benkaddour, T. Benhadda, Thiophene derivatives as effective inhibitors for the corrosion of steel in 0.5M H₂SO₄, *J. Appl. Electrochem.*, 35 (2004) 134-138.
- [42] S. Martinez, I. Stern, *Appl. Surf. Sci.*, 199(1-4) (2002) 83-89.
- [43] M. Dahmani, A. Et-Touhami, S.S. Al-Deyab, B. Hammouti, A. Bouyanzer, *Int. J. Electrochem. Sci.*, 5 (2010) 1060-1069.
- [44] S. Aloui, I. Forsal, M. Sfaira, M. EbnTouhami, M. Taleb, M. Filali Baba, M. Daoudi, *Port. Electrochim. Acta*, 27 (5) (2009) 599.
- [45] M. Rbaa, F. Benhiba, I.B. Obot, H. Oudda, I. Warad, B. Lakhrissi, A. Zarrouk, *J. Mol. Liq.*, 12 (276) (2018) 120-133.
- [46] M. Rbaa, H. Lgaz, Y. El Kacimi, B. Lakhrissi, F. Bentiss, A. Zarrouk, *Materials Discovery*, 12 (2018) 43–54.